

Francesco Baldi,¹ Silvia Agnelli,² Luca Andena,³ Bamber R. K. Blackman,⁴ Leonardo Castellani,⁵ Patricia M. Frontini,⁶ Jaroslav Kučera,⁷ Lucien Laiarinandrasana,⁸ Alessandro Pegoretti,⁹ Alicia Salazar,¹⁰ and Laurent Warnet¹¹

Determination of the Fracture Resistance of Ductile Polymers: The ESIS TC4 Recent Experience

Reference

F. Baldi, S. Agnelli, L. Andena, B. R. K. Blackman, L. Castellani, P. M. Frontini, J. Kučera, L. Laiarinandrasana, A. Pegoretti, A. Salazar, and L. Warnet, "Determination of the Fracture Resistance of Ductile Polymers: The ESIS TC4 Recent Experience," *Materials Performance and Characterization* 9, no. 5 (2020): 675–687. <https://doi.org/10.1520/MPC20190175>

ABSTRACT

Round-robin (RR) tests carried out under the direction of the Technical Committee 4, "Polymers, Polymer Composites and Adhesives," of the European Structural Integrity Society (ESIS TC4) showed that the multispecimen methodology employed for the construction of the crack growth resistance curve (J vs crack extension, Δa) of polymers often does not provide reliable data because of the uncertainties associated with the measurement of Δa . With this in mind, the ESIS TC4 attention has been more recently focused on the analysis of a testing scheme based on the load separation criterion, which does not require the measurement of Δa . With the aim to employ this new approach into a standardized procedure, the degree of reproducibility of the results obtainable with the application of this testing scheme to ductile polymers has been assessed by means of multilaboratory RR testing exercises that started in 2011. An ESIS TC4 reference draft protocol was prepared and 10 laboratories participated in the RR activities. The present work describes the load separation criterion-based testing procedure recently examined by ESIS TC4 and gives a summary of the results obtained in the RR activities, which appear encouraging.

Keywords

J-integral, load separation criterion, fracture resistance, ductile polymers

Manuscript received July 20, 2019; accepted for publication January 3, 2020; published online July 15, 2020. Issue published October 15, 2020.

¹ Dipartimento di Ingegneria Meccanica e Industriale, Università degli Studi di Brescia, Via Branze 38, 25123 Brescia, Italy (Corresponding author), e-mail: francesco.baldi@unibs.it, <https://orcid.org/0000-0001-6174-4474>

² Dipartimento di Ingegneria Meccanica e Industriale, Università degli Studi di Brescia, Via Branze 38, 25123 Brescia, Italy

³ Dipartimento di Chimica, Materiali e Ingegneria Chimica "G. Natta," Politecnico di Milano, Piazza Leonardo da Vinci 32, 20133 Milano, Italy

⁴ Department of Mechanical Engineering, Imperial College London, South Kensington Campus, London SW7 2AZ, UK

⁵ Versalis S.p.A., Basic Chemicals and Plastics Research Center, Via Taliercio 14, 46100 Mantova, Italy

⁶ Universidad Nacional de Mar del Plata, Instituto de Investigaciones en Ciencia y Tecnología de Materiales (INTEMA), Colón 10850 Mar del Plata, Argentina (B7606BVZ)

⁷ Unipetrol RPA, s.r.o. - Polymer Institute Brno, odštěpný závod, Tkalcovská 36/2, 602 00 Brno, Czech Republic

⁸ MINES ParisTech, PSL Research University, MAT-Centre des Matériaux, CNRS UMR 7633, BP 87, Evry Cedex, France

⁹ Dipartimento di Ingegneria Industriale, Polo Scientifico e Tecnologico "F. Ferrari," Università degli Studi di Trento, Via Sommarive 9, 38123 Trento, Italy

¹⁰ Grupo de Durabilidad e Integridad Mecánica de Materiales Estructurales (DIMME), Escuela Superior de Ciencias Experimentales y Tecnología, Universidad Rey Juan Carlos, C/ Tulipán s/n, Móstoles, 28933 Madrid, Spain

¹¹ Faculty of Engineering Technology, University of Twente, PO Box 217, 7500 AE Enschede, the Netherlands

Introduction

To determine the low-rate fracture resistance of ductile polymers, for which the application of standard linear elastic fracture mechanics (LEFM) tests fails, the material crack growth resistance (J_R) curve (J vs crack extension, Δa), developed within the frame of elastic-plastic fracture mechanics (EPFM), is generally employed. This is usually constructed by means of a multispecimen approach (procedure developed by ESIS TC4,¹ that is, the Technical Committee 4, "Polymers, Polymer Composites and Adhesives," of the European Structural Integrity Society,² and ASTM D6068-10(2018), *Standard Test Method for Determining J-R Curves of Plastic Materials*³). Specific ESIS TC4 round-robin (RR) tests showed that the uncertainties associated with the measurement of Δa often make this approach unreliable. Furthermore, in many cases, an initiation fracture resistance parameter, J_{Ic} , cannot be obtained. With this in mind, the attention of ESIS TC4 has been recently paid to the analysis of a single-specimen testing scheme based on the load separation criterion (LSC), which does not require the measurement of Δa (see Agnelli et al.⁴). This approach would (i) allow the determination of a material initiation fracture resistance parameter, $J_{I,lim}$, and (ii) provide a rough measure of Δa produced during the fracture test in the plastic region. In order to assess the degree of reproducibility of the results obtainable with the application of this method, in view of its possible employment in a standardized procedure, a multilaboratory activity was begun in September 2011 under the direction of ESIS TC4, with Università degli Studi di Brescia (Italy) as the coordinating laboratory. Ten laboratories (indicated in the authors' affiliation list) participated in this activity, which was organized on three consecutive RR testing exercises (RR1 to RR3). RR1 consisted in a preliminary work aimed at setting the key points for the preparation of the reference draft testing protocol,⁵ which was prepared in 2013 and then further reviewed in 2015. In RR2 and RR3, this drafted protocol (called RR protocol hereafter) was applied to the fracture characterization of polymeric materials that exhibit a ductile behavior but different degrees of stiffness and strength (from standard tensile tests). The outcomes were used to enhance the robustness of the method and to improve the protocol itself. The examined materials were as follows: an acrylonitrile-butadiene-styrene (ABS) and a high-impact polystyrene (HIPS) in RR2 (the RR2 results are presented in Agnelli et al.⁴); and a rubber-toughened polybutylene terephthalate (RT-PBT) and a linear low-density polyethylene (LLDPE) in RR3. The present work describes the LSC-based testing procedure examined by ESIS TC4 and gives a summary of the results obtained during the RR activities.

The LSC-based Testing Method

The method described in the RR protocol,⁵ founded on the LSC proposed by Ernst, Paris, and Landes,⁶ was derived from Sharobeam and Landes' works published in the early 90s on metals.^{7,8} The LSC assumes that, for a defined specimen geometry, material, and constraint, the load, P , recorded in a fracture test in the plastic region can be mathematically represented as the product of two independent functions, as equation (1) shows:

$$P = G\left(\frac{b}{W}\right) \cdot H\left(\frac{u_{pl}}{W}\right) \quad (1)$$

where $G(b/W)$ and $H(u_{pl}/W)$ are the geometry and the material deformation functions, respectively, W is the specimen width, b the specimen uncracked ligament length (that is

$W - a$, with a that indicates the crack length), and u_{pl} is the plastic displacement (that is the plastic component of the total displacement, u). The applicability of the LSC to polymeric materials, during both blunting and crack propagation phase, has been demonstrated (see Bernal, Cassanelli, and Frontini,^{9,10} Bernal, Montemartini, and Frontini,¹¹ Morhain and Velasco,^{12,13} Salazar and Rodríguez,¹⁴ and Baldi, Agnelli, and Riccò¹⁵).

The testing method described in the RR protocol⁵ is based on the construction of the “load separation parameter curve,” i.e., the S_{sb} curve, from tests in single edge-notched bending (SE(B)) configuration (see **fig. 1**). It requires the execution of two tests: on a sharp-notched (sN) specimen and on a blunt-notched (bN) specimen. A schematic representation of a sharp and of a blunt notch is shown in **figure 1**. In the sN specimen, fracture propagation occurs, whereas in the bN specimen, crack growth is hindered. From the load, P , versus displacement, u , curves obtained from quasi-static tests on sN and bN specimens, the separation parameter, S_{sb} , is determined as follows:

$$S_{sb}(u_{pl}) = \left. \frac{P_s}{P_b} \right|_{u_{pl}} \quad (2)$$

where P_s and P_b are load values read on P versus u_{pl} curves of the sN and bN specimens, respectively, at a given value of plastic displacement, u_{pl} , which, in the protocol examined here, is determined for each specimen as:

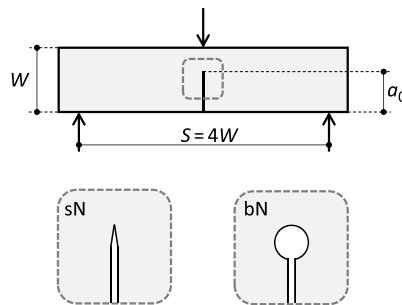
$$u_{pl} = u - P \cdot C_0 \quad (3)$$

where C_0 is the initial elastic compliance of the specimen. With reference to u_{pl} determined according to equation (3), that is from C_0 , it is worth pointing out that (i) for the sN specimen in the crack propagation phase, u_{pl} data assume a nominal character in consideration of the fact that the true u_{pl} data should be evaluated from the actual compliance, C , that increases during the crack growth phase but is not known (the determination of C would require test interruption and the measurement of Δa [see Appendix, where true u_{pl} data determined from C have been used for the verification of the LSC validity for RT-PBT]); (ii) in consideration of the viscoelastic nature of polymeric materials, u_{pl} represents the “non-elastic” component of the total displacement, u , which for these materials is in general the sum of three contributions: elastic, viscoelastic, and plastic. Preliminary investigations specifically carried out by the laboratory of Brescia showed that, to the aims of the testing method examined here (RR protocol⁵), u_{pl} data evaluated from C_0 can be successfully used.

It is expected that the S_{sb} curve, that is, S_{sb} plotted against u_{pl} shows a “plateau” region, whereas S_{sb} maintains an almost constant value ($S_{sb,plateau}$), followed by a decreasing S_{sb} region. The former region corresponds to the crack blunting phase, whereas the latter region corresponds to the crack propagation phase in the fracture process of the sN specimen. The point between these two regions (called the limit point), at $u_{pl} = u_{pl,lim}$, corresponds to fracture initiation (or pseudo-initiation, especially considering that for ductile polymers fracture initiation can be

FIG. 1

Schematic representation of a SE(B) specimen. S is the span. Sharp (of a sharp-notched, sN, specimen) and blunt (of a blunt-notched, bN, specimen) notches are also represented; the blunt notch is a keyhole type.



a complex progressive process¹⁶). J-integral value at $u_{pl,lim}$, that is $J_{I,lim}$, which can be taken as a material pseudo-initiation fracture resistance parameter in place of the more conventional $J_{0.2}$ computed by the J_R curve (see the ESIS TC4 procedure¹), is evaluated as follows:

$$J_{I,lim} = \frac{2 \cdot U_{lim,c}}{B \cdot (W - a_0)} \quad (4)$$

where $U_{lim,c}$ is the energy up to the limit point, corrected for indentation (see the ESIS TC4 procedure¹), and B , W , and a_0 are the thickness, width, and initial crack length of the sN specimen, respectively.

Furthermore, the normalized separation parameter curve (R_S curve), i.e., R_S versus u_{pl} , is traced (R_S is obtained as the ratio of S_{sb} over $S_{sb,plateau}$), and the parameter m_S is determined in the region of fracture propagation as follows:

$$m_S = - \left. \frac{dR_S}{du_{pl}} \right|_{u_{pl} > u_{pl,lim}} \quad (5)$$

It has been shown⁴ that parameter m_S , which is a specimen characteristic (i.e., dependent on both specimen geometry and material), provides an indication of the crack advancement produced per unit of u_{pl} and could be used, as a “ductility index,” to classify the fracture propagation processes by the amount of crack growth occurring within the plastic region. The higher the value of m_S , the higher the Δa per unit of u_{pl} ; if $m_S \rightarrow 0$, the process is governed by crack blunting.

Further details concerning this methodology can be found in Agnelli et al.⁴ and in the RR protocol.⁵

Experimental

Materials ABS, HIPS, and LLDPE were provided by Versalis SpA (Mantova, Italy), whereas RT-PBT was provided by Radici Novacips SpA (Villa d'Ogna, Bergamo, Italy). **Table 1** reports the supply form of the materials, their basic mechanical properties and the nominal dimensions of the SE(B) specimens used in the RR fracture tests. For ABS, HIPS, and RT-PBT the fracture resistance, $J_{0.2}$ data are also indicated. They were obtained from the J_R curve constructed by the application of the ESIS TC4 multispecimen approach¹ on specimens having the same geometry and dimensions of the RR tests (for ABS and HIPS, $J_{0.2}$ data are from Agnelli et al.⁴; for RT-PBT, the J_R curve is reported in the Appendix).

Each laboratory prepared and tested at least three sN and one bN specimens for each of the materials considered. The notching techniques were freely chosen by the laboratory, following the guidelines provided by the RR protocol.⁵ For LLDPE, two sets of specimens (#a and #b in **Table 1**) that differed in size were examined. This was done in order to explore, for this very ductile polymer (which also showed the lowest degrees of stiffness and

TABLE 1

Supply form of the materials examined and their basic mechanical properties (Young's modulus, E , and tensile yield stress, σ_y); nominal dimensions of SE(B) specimens used in the fracture tests; and $J_{0.2}$ data

Material (RR)	Supply Form	Basic Mechanical Properties ^a		SE(B) Specimen Dimensions ^b			
		E (MPa)	σ_y (MPa)	B (mm)	W (mm)	a_0 (W)	$J_{0.2}$ (kJ/m ²)
HIPS (RR2)	Injection-molded dumbbells ^c	1,760	18	4	10	0.6	2.84
ABS (RR2)	Six-mm-thick compression molded plates	2,500	44	6	12	0.6	5.71
RT-PBT (RR3)	Injection-molded dumbbells ^c	1,450	31	4	10	0.6	6.58
LLDPE ^d (RR3)	Ten-mm-thick injection-molded plates	250	8	10	10 (#a)	0.6	- ^e
					20 (#b)		

Note: ^a From quasi-static tests at room temperature. ^b B , thickness; W , width; a_0 , initial crack length (in bN specimen, notch tip radius of 1 mm); span used in fracture tests, $S = 4W$ (ref. to **fig. 1**). ^c According to ISO 3167:2014, *Plastics – Multipurpose Test Specimens*; central narrow portion (with dimensions of $80 \times 10 \times 4$ mm³) used for SE(B) specimen preparation. ^d Two sets of SE(B) specimens (#a and #b) used. ^e Not measured (J_R curve not constructed).

strength among the materials examined), how the results obtainable by the application of the RR protocol could be affected by the specimen size (geometrical constraint). All the experiments were performed by means of universal testing machines at $\approx 23^\circ\text{C}$ and with a crosshead rate of 1 mm/min. The data were processed according to the RR protocol,⁵ and the results (consisting of the S_{sb} curve and data from $J_{I,lim}$ and m_s , for each sN specimen tested) were sent to the laboratory of Brescia for the comparative analysis.

The applicability of the LSC to styrenic polymers and polyolefins has been examined in several literature works; in contrast, to the best of the authors' knowledge, the applicability of the LSC to RT-PBT has never been checked. Therefore, before starting the RR activity on the RT-PBT, the validity of the LSC has been experimentally verified (see Appendix).

Results and Discussion

Figure 2A and **2B** report $J_{I,lim}$ and m_s results, respectively, for the various materials examined. Each datum reported is the mean value obtained by averaging all the data from the various laboratories. The datum considered for each laboratory is the average of the data obtained from the various sN specimens tested at the laboratory.

The degree of repeatability of the results within the same laboratory was generally higher than that of reproducibility (represented by the data of standard deviation reported in **fig. 2**). Results with a very high degree of repeatability could be obtained, and this emerges clearly from **figure 3A–E**, in which the R_s curves of different nominally identical sN specimens of a given material, obtained at a given (selected) laboratory, are compared (the curves are vertically shifted for clarity). **Figure 3A** refers to specimens of HIPS tested at Laboratory 10; **figure 3B** refers to specimens of ABS tested at Laboratory 11; **figure 3C** refers to RT-PBT tested at Laboratory 1 (the R_s curves are reported both shifted and not); **figure 3D** and **3E** refers to LLDPE specimens with size #a and #b, respectively, tested at Laboratory 6 (laboratory numbers are in accordance with the authors' affiliation list). In **figure 3A** and **3B**, the R_s curve indicated with an asterisk was built at Brescia based on the raw data provided by the laboratory that performed the tests. This was done, within the RR2 activities, just to check whether the data processing procedure described in the RR protocol⁵ had been properly applied by the laboratory. **Figure 3C**

FIG. 2 Mean values (\pm standard deviation) of (A) $J_{I,lim}$ and (B) m_s for the various materials examined, which were obtained by averaging all the (mean) data from the various laboratories (refer to **Table 1** for the dimensions of the specimens). Values in parentheses indicate the standard deviation expressed as a percentage of the corresponding mean value. For LLDPE, valid $J_{I,lim}$ data could not be obtained (see text). Data with an asterisk are from Agnelli et al.⁴

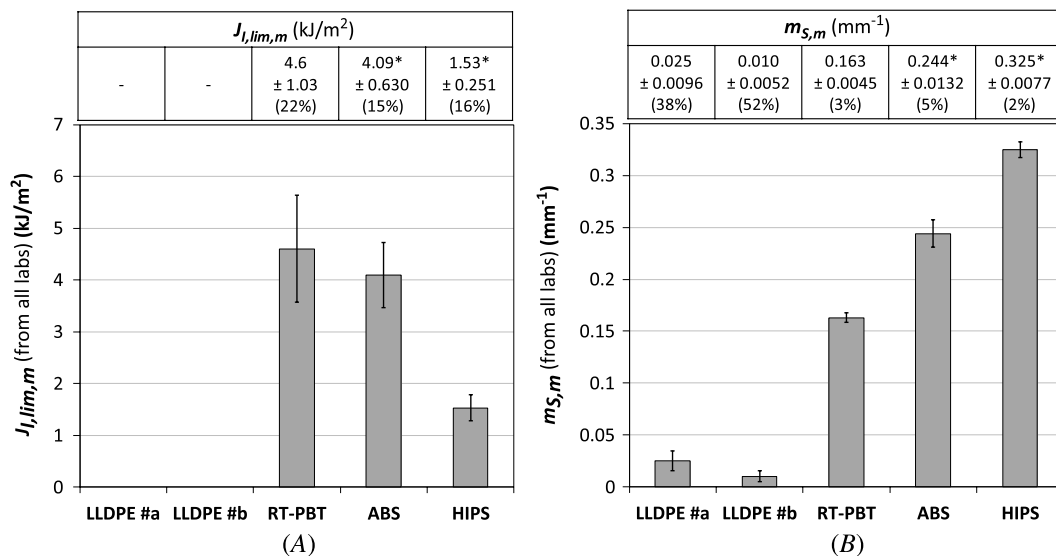
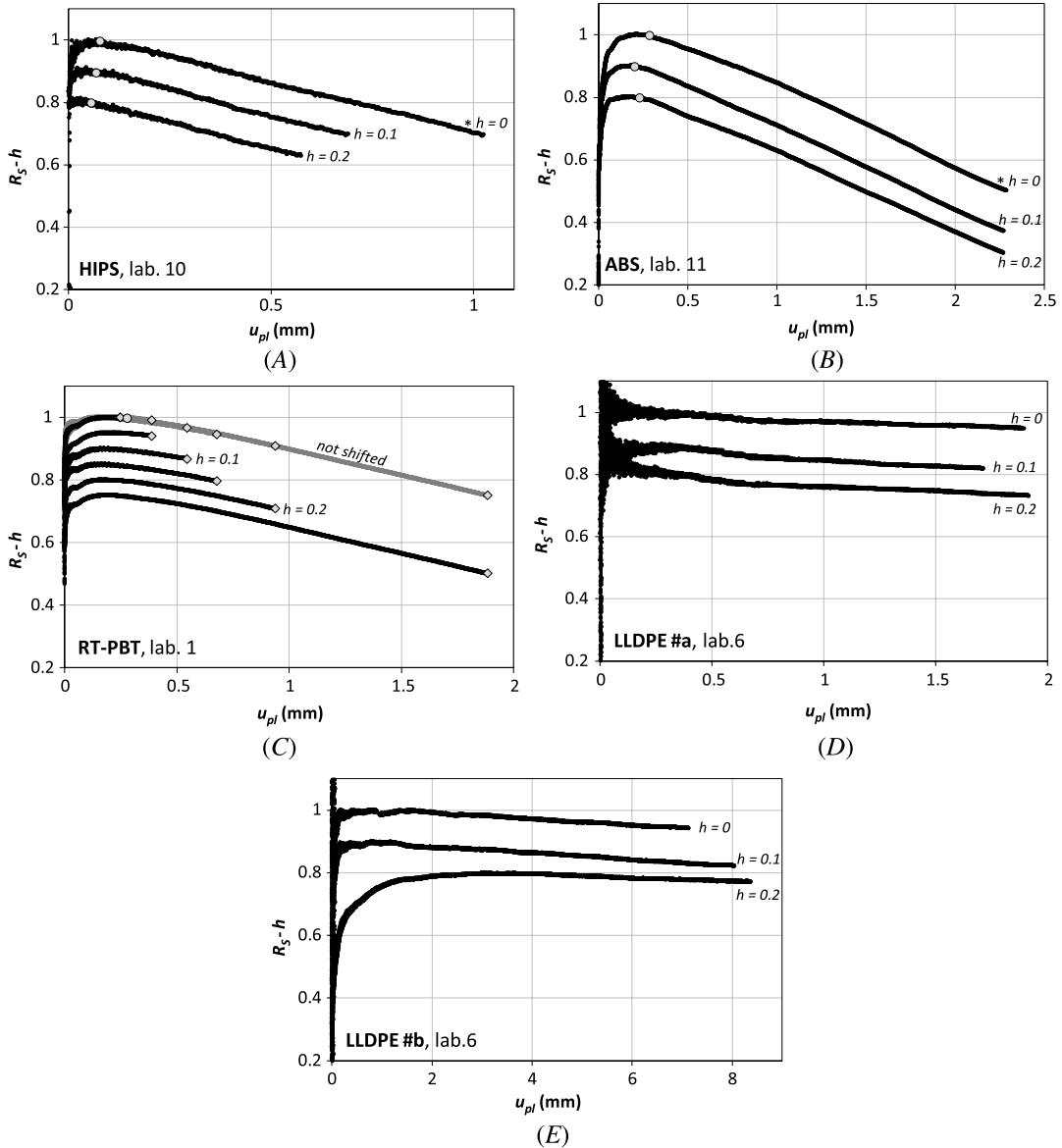


FIG. 3 R_S curves of different nominally identical sN specimens of (A) HIPS, from Laboratory 10; (B) ABS, from Laboratory 11; (C) RT-PBT, from Laboratory 1; (D) and (E) LLDPE, #a and #b, respectively, from Laboratory 6. The curves are vertically shifted by an h -factor. In (A), (B), and (C), the gray circles indicate the limit point. In (C), the curves are also represented as not shifted (in gray); rhomb indicates the final point (that is, the point at which the test was interrupted). See text for explanation of the asterisk in (A) and (B).



shows the R_S curves obtained at Brescia (Laboratory 1) from six sN specimens of RT-PBT, tested up to different levels of displacement (the rhomb indicates, for each sN specimen test record, the point at which the fracture test was interrupted, i.e., the final point). If not shifted vertically, these curves overlap well, and they practically draw one single curve in which the plateau region that extends up to the limit point is clearly visible. For the LLDPE, the degree of repeatability of the results was generally lower with respect to the other materials, as can be observed in [figure 3E](#). This is related to the fact that LLDPE was largely the most difficult-to-characterize material. Even if relatively high displacement values were reached (especially with size #b; refer to [fig. 3E](#)), which is also necessary

in consideration of the low Young's modulus of the material, reliable plateau regions could not be clearly identified in the S_{sb} curves of the sN specimens tested. This indicates that, in the tests on the SE(B) specimens of the LLDPE examined herein, the crack blunting phase could not be distinguished from the crack propagation phase, and valid initiation fracture resistance data ($J_{I,lim}$) could not be obtained.

Focusing attention on HIPS, ABS, and RT-PBT, for which data of both $J_{I,lim}$ and m_S have been obtained, it can be observed that the degree of reproducibility for the latter data is higher than that for the former data (see [fig. 2A](#) and [2B](#)). This suggests that, with respect to the fracture propagation phase, which is what the m_S parameter refers to, fracture initiation/early stages of crack growth, which is what $J_{I,lim}$ refers to, are less reproducible (at a macroscopic scale). Examination of the results collected from the various laboratories seems to indicate that the scattering observed for the $J_{I,lim}$ data is related to a combination of both testing and data analysis aspects.

(i) In relation to testing, the results suggest that the quality of the notch of the sN specimens played an important role. As underlined by Salazar et al.¹⁷ and Martínez et al.,¹⁸ the influence of the sharp notch quality on the determination of the initiation fracture resistance of polymeric materials, in plane strain conditions via both LEFM and EPFM methods, is still not fully understood. Within ESIS TC4, an RR exercise aimed at identifying the most suitable notching technique for the preparation of the notched specimens for the execution of plane strain LEFM tests is currently underway.² The outputs of this RR activity will be used, at a later stage, as the basis for an investigation into the effects of the sharp notch quality in J-testing of ductile polymers.

(ii) With regard to data analysis, the results clearly point out that a crucial role is played by the determination of the initial specimen compliance, C_0 . In addition, the procedure described in the RR protocol⁵ for the identification of the limit point on the S_{sb} curve can be further improved. Within ESIS TC4, specific activities aimed at carefully examining these aspects are in progress. More specifically, an RR exercise aimed at evaluating the reproducibility degree of the data of initial elastic compliance, C_0 , of SE(B) specimens of polymeric materials that exhibit a ductile behavior is currently underway.

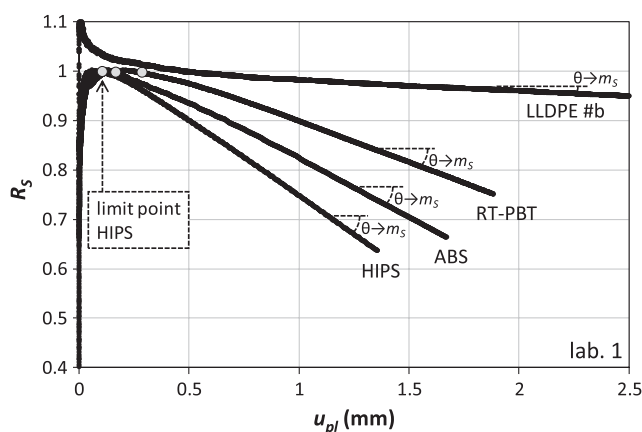
Even if the degree of scattering observed for $J_{I,lim}$ data is higher than that of m_S data, it can be acceptable within the field of fracture mechanics testing. Interestingly, not only for HIPS and ABS (as already pointed out by Agnelli et al.⁴) but also for RT-PBT, the $J_{I,lim}$ value is lower than the value of the technological $J_{0.2}$ parameter read on the J_R curve (see [Table 1](#) and Appendix). This suggests that the LSC-based approach examined here is able to provide data of fracture resistance that is more conservative with respect to $J_{0.2}$. It is worth noting, also, that for each material, the value of $J_{I,lim}$ verified the size criteria proposed in the ESIS TC4 protocol¹ for critical J-values, and this indicates that the $J_{I,lim}$ values refer to a plane strain state at the crack tip and that plasticity in the ligament is not excessive.

[Figure 4](#) shows the R_S curves constructed at the laboratory of Brescia in compliance with the RR protocol, for the SE(B) specimens of the different materials examined (one single curve for each material). For LLDPE, only the curve of size #b, which refers to specimens with a width-to-thickness ratio closer to those of the specimens of the other materials, is reported. The differences among the fracture processes of the various specimens emerge clearly. Interestingly, by comparing the R_S curves of RT-PBT and HIPS (that is, at fixed specimen dimensions, see [Table 1](#)), it can be observed that the extension of the plateau region of the curve is larger for the former than for the latter. This indicates that the higher fracture resistance obtained for RT-PBT with respect to HIPS ($J_{I,lim}$ of RT-PBT is ≈ 3 times that of HIPS, see [fig. 2A](#)) can be related also to the fact that the blunting-to-fracture transition, in the fracture process of a sN specimen, occurs at a level of u_{pl} that is higher for the former than for the latter.

The analysis of the fracture process based on the application of the RR protocol⁵ brings to light, for the LLDPE, a behavior remarkably different from that of the other ductile polymeric materials examined. For the construction of the R_S curve of LLDPE, in absence of a reliable $S_{sb,plateau}$ following the protocol,⁵ the value of S_{sb} at $u_{pl} = 0.5$ mm was used in place of $S_{sb,plateau}$. The low values of m_S obtained (see [fig. 2B](#)) clearly suggest that the process is governed by blunting: irrespective of the specimen size considered, either #a or #b, crack growth produced per unit of u_{pl} is very small. The high degree of scattering obtained for m_S data suggests that its fracture process is not easily reproducible, contrary to what has been observed for the other materials for which standard deviations of m_S are quite small. This is one of the reason why a reliable J_R curve could not

FIG. 4

R_S curves obtained at Laboratory 1 from the fracture tests on the various materials examined (one curve for each material; refer to [Table 1](#) for the dimensions of the specimens). Gray circles indicate the limit point on the R_S curves of HIPS, ABS, and RT-PBT. For each curve, m_S is also represented.



be constructed for this material (see [Table 1](#)), for which, furthermore, valid data of Δa could not be obtained by the inspection of the fracture surface produced. Even if valid fracture resistance data ($J_{I,lim}$) have not been determined for LLDPE, the testing procedure examined here was able to highlight, through m_S determination, that a testing scheme based on the propagation of a crack cannot be successfully applied to this material, working on SE(B) specimens with dimensions as in [Table 1](#). It would be necessary to use different specimen geometry/dimensions or to resort to another testing approach that does not require the use of precracked specimens, such as cutting tests (see Patel, Blackman, and Williams¹⁹).

The results obtained for RT-PBT and LLDPE, in RR3, strengthen the idea that was outlined by Agnelli et al.⁴: to attribute a key role to the m_S parameter in the fracture characterization of ductile polymers. The uncertainties associated with the measurement of Δa , which impair the construction of the J_R curve, can have various causes: instrumental, methodological, or related to the intrinsic fracture behavior of the material. The measurement of Δa is typically based on the optical analysis of the fracture surface generated during the test, and the greatest difficulty is associated with the correct evaluation of the crack front that defines the region on the fracture face characteristic of actual crack growth. More specifically, the obtainment of reliable Δa data can be particularly arduous if, depending on the material, the crack growth produced in the fracture test is very limited or it is overshadowed by blunting (that was the case of the LLDPE examined here), or it is complicated by the occurrence of specific phenomena, such as with multiple cracking. Results obtained in the RR exercise reported here show that the application of the RR protocol,⁵ which in principle requires only two tests, is effective at distinguishing between, using the m_S parameter, fracture processes governed by blunting ($m_S \rightarrow 0$) and processes in which the crack growth actually occurs (with $m_S > 0$). With this in mind, m_S might be used as a key parameter in a criterion to check a priori if the application of the multispecimen approach for J_R curve construction (founded on the measurement of Δa) to specimens with given geometry and dimensions is likely to fail. More specifically, with reference to SE(B) specimens (that is, the testing geometry considered in this work), a critical value of m_S ($m_{S,c}$) might be fixed and used according to the following scheme:

- The LSC-based procedure is applied to a ductile polymer in the form of specimens with given dimensions, and the values of m_S and $J_{I,lim}$ are determined (the possibility that the S_{sb} plateau region is not clearly identified and, therefore, that $J_{I,lim}$ is not evaluated cannot be ruled out);
- If $m_S > m_{S,c}$, then the value of $J_{I,lim}$ obtained is taken as the fracture resistance of the material (if the size criteria proposed for critical J-values in the ESIS TC4 protocol¹ are verified), and the application of the multispecimen approach for J_R curve construction might be attempted;

- If $m_S \leq m_{S,c}$, then $J_{I,lim}$ (if determined) cannot be considered valid, and the multispecimen approach for J_R curve construction cannot be applied; in this case, either the specimen dimensions are modified and new LSC-based tests performed or a different testing scheme that is not based on the use of precracked specimens (e.g., cutting tests¹⁹) is employed.

Of course, the analysis of the source of the errors in the measurement of Δa deserves a special consideration. To this aim, specific ESIS TC4 activities are currently being developed. More specifically, interlaboratory RR exercises focused on the instrumental and methodological aspects related to the optical analysis of the fracture surface for Δa evaluation will be organized. The possibility to resort to noncontact techniques (e.g., digital image correlation) for the indirect monitoring of crack advancement during the fracture test will also be considered.

Conclusions

The results obtained in the ESIS TC4 RR activity on the use of LSC in J-testing of ductile polymers are encouraging. The method under development has been successfully applied to ductile polymers that exhibit different degrees of stiffness and strength (ABS, HIPS, RT-PBT, and LLDPE). It allows determination of a material pseudo-initiation fracture resistance parameter ($J_{I,lim}$) as well as a crack propagation parameter (m_S). The results suggest that this latter parameter can play a key role in a criterion to check a priori if the multispecimen approach for J-testing (the ESIS TC4 procedure¹ or the ASTM D6068-10(2018)³) applied to a ductile polymer (with given specimen geometry and dimensions) is likely to fail. The RR activity is still in progress, and special attention is being given to this latter outcome.

ACKNOWLEDGMENTS

The authors are grateful to Versalis SpA (Mantova, Italy) and Radici Novacips SpA (Villa d'Ogna, Bergamo, Italy) for kindly supplying the materials tested in this study.

Appendix: Construction of J_R Curve and Verification of the LSC Validity for RT-PBT

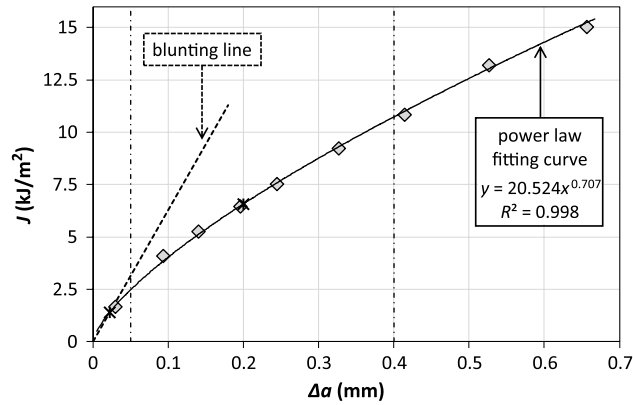
The J_R curve was constructed according to the ESIS TC4 procedure.¹ The same specimen geometry and dimensions (sN specimen, Table 1) and testing conditions (crosshead rate and temperature) of the RR tests were used. Figure A.1 shows the experimental (Δa ; J) data points fitted by the power law best-fitting curve, the exclusion lines, and the blunting line, which was traced according to the following analytical expression:

$$J = 2 \cdot m \cdot \sigma_y \cdot \Delta a \quad (A.1)$$

where a value of $m = 1$ was used. The points on the J_R fitting curve corresponding to $J_{0.2}$ (that is at $\Delta a = 0.2$ mm) and to J_{bl} (that is, at the intersection with the blunting line) are also indicated. The value of $J_{0.2}$ is reported in Table 1; J_{bl} resulted in 1.39 kJ/m².

As underlined by Sharobeam and Landes,⁸ if the load is separable during the fracture propagation phase, S_{sb} data evaluated at different levels of u_{pl} (when the crack is growing) should lie on one single curve if plotted against the actual values of b/W . For such verification, the sN specimens that have the highest geometrical similarity among the specimens tested for the construction of the J_R curve (which are those whose R_S curves are reported in fig. 3C) were selected, and their P versus u curves and Δa data at the final point were considered. In this analysis, differently from what was done for the application of the RR protocol, the actual values of u_{pl} at the final points—where the crack length, a , is $a_0 + \Delta a$ —were used. These u_{pl} data were evaluated from the actual specimen elastic compliance, $C(a/W)$, which was indirectly calculated by using the following expression²⁰:

FIG. A.1 J_R curve of RT-PBT, constructed according to the ESIS TC4 procedure.¹ The experimental (Δa ; J) data points (rhomb), the power law best-fitting curve (solid line), the exclusion lines (vertical dash-dot lines), the blunting line (dashed line), and the points on the fitting curve corresponding to J_{bl} and $J_{0.2}$ (asterisk)—see text—are indicated. The equation of the power law best-fitting curve and the correlation coefficient of the fitting (R^2) are also reported.



$$C(a/W) = \frac{2 \cdot [f(a/W)]^2 \cdot \Phi(a/W)}{E_{fract} \cdot B} \quad (A.2)$$

where $f(a/W)$ and $\Phi(a/W)$ are tabulated functions.²¹ The value of E_{fract} with a result of $1,400 \pm 50$ MPa, was previously determined by applying equation (A.2)—inverted—to the data of a_0/W and C_0 (corrected by taking into account the specimen indentation compliance; see the ESIS TC4 procedure¹) of all the specimens used for the J_R curve construction.

Figure A.2 shows the data points (b/W ; S_{sb}) corresponding to the final points of the sN specimens test records considered. For S_{sb} determination, the bN specimen test record of the RR experiments was used. These data points (b/W ; S_{sb}), which are associated with different values of u_{pb} , draw a single trend, and this

FIG. A.2 Separation parameter, S_{sb} , evaluated at the final point of each sN specimen test record of RT-PBT examined (R_S curves in fig. 3C), plotted against the corresponding value of the actual remaining ligament length divided by the specimen width, b/W (rhomb). The dashed line indicates the power law best-fitting curve forced to the experimental (b/W ; S_{sb}) data at the final points. The theoretical point with $S_{sb} = 1$ (asterisk)—see text—is indicated. The equation of the fitting curve and the correlation coefficient of the fitting (R^2) are also reported.

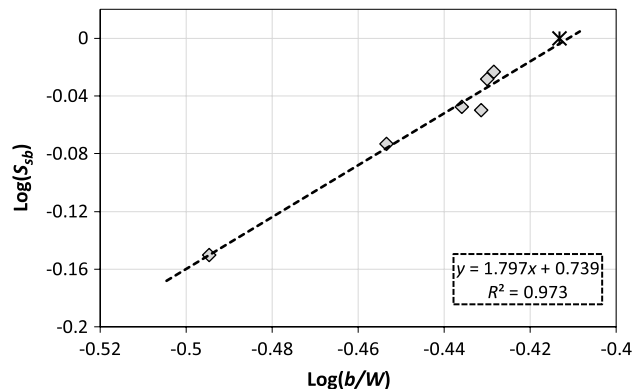
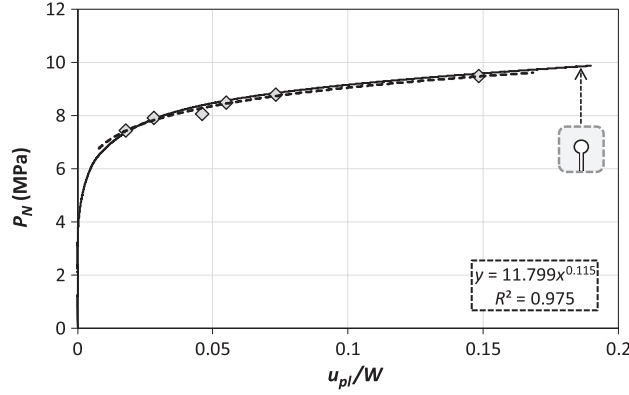


FIG. A.3 Normalized load, P_N , calculated at the final point of each sN specimen test record of RT-PBT examined (R_S curves in [fig. 3C](#)), plotted against the corresponding value of u_{pl}/W (rhomb). The dashed line indicates the power law best-fitting curve forced to the experimental data (u_{pl}/W ; P_N), whose equation and correlation coefficient (R^2) are also reported. The solid line indicates the P_N versus u_{pl}/W curve obtained from the bN specimen of RT-PBT.



indicates that u_{pl} has no contribution on the value of S_{sb} and, therefore, that the LSC is valid during crack propagation. For SE(B) configuration, the geometry function, $G(b/W)$, can be expressed as (see Sharobeam and Landes⁷) follows:

$$G\left(\frac{b}{W}\right) = \left(\frac{b}{W}\right)^{\eta_{pl}} \quad (\text{A.3})$$

Therefore, a power law best-fitting curve—linear in the bilogarithmic plot of [figure A.2](#)—was forced on the fracture propagation data points. According to equation (A.3), the slope of the fitting line is η_{pl} , which results in 1.8. The difference between this value and the theoretical value of 2 derived by Rice, Paris, and Merkle²² for η_{pl} and widely adopted in literature, is very similar to those observed in other literature works in which values of η_{pl} were determined experimentally (see Sharobeam and Landes,⁸ Bernal, Montemartini, and Frontini,¹¹ Baldi, Agnelli, and Riccò,¹⁵ and Baldi and Riccò²³). Interestingly, the fitting curve passes very closely to the theoretical point at $S_{sb} = 1$, which corresponds to a crack length in the sN specimen equal to the stationary crack length of the bN specimen.

The material deformation function, $H(u_{pl}/W)$, that characterizes the material during fracture propagation was then constructed—see equation (1). Following Sharobeam and Landes,⁸ it was built by referring to the normalized load, P_N , that was evaluated as follows:

$$P_N\left(\frac{u_{pl}}{W}\right) = \frac{P\left(\frac{u_{pl}}{W}\right)}{B \cdot W \cdot G\left(\frac{b}{W}\right)} \quad (\text{A.4})$$

where $\eta_{pl} = 1.8$ was used in the expression of $G(b/W)$. [Figure A.3](#) shows the values of P_N calculated at the final point of each sN specimen test record, plotted against the corresponding values of u_{pl}/W . A power law best-fitting curve was forced to the experimental data points (this curve is known as “material key curve”; see Agnelli et al.²⁴). In [figure A.3](#), the P_N versus u_{pl}/W curve obtained from the P versus u curve of the bN specimen, which exhibits only blunting, is also reported. Interestingly, the material deformation function during the fracture propagation phase has the same form as during the blunting phase, and this is the experimental verification of the assumption on which the LSC is founded.

References

1. G. E. Hale and F. Ramsteiner, "J-Fracture Toughness of Polymers at Slow Speed," in *Fracture Mechanics Testing Methods for Polymers, Adhesives and Composites, European Structural Integrity Society Publication 28*, ed. D. R. Moore, A. Pavan, and J. G. Williams (Oxford, UK: Elsevier, 2001), 123–157.
2. European Structural Integrity Society, "ESIS Home Page," European Structural Integrity Society, <http://web.archive.org/web/20200118124803/https://www.structuralintegrity.eu/>
3. *Standard Test Method for Determining J-R Curves of Plastic Materials*, ASTM D6068-10 (2018) (West Conshohocken, PA: ASTM International, approved October 1, 2018), <https://doi.org/10.1520/D6068-10R18>
4. S. Agnelli, F. Baldi, B. R. K. Blackman, L. Castellani, P. M. Frontini, L. Laiarinandrasana, A. Pegoretti, M. Rink, A. Salazar, and H. A. Visser, "Application of the Load Separation Criterion in J-Testing of Ductile Polymers: A Round-Robin Testing Exercise," *Polymer Testing* 44 (July 2015): 72–81, <https://doi.org/10.1016/j.polymertesting.2015.03.019>
5. S. Agnelli and F. Baldi, *A Testing Protocol for the Construction of the Load Separation Parameter Curve for Plastics, ESIS TC4 Communication* (European Structural Integrity Society, 2015).
6. H. A. Ernst, P. C. Paris, and J. D. Landes, "Estimations on J-Integral and Tearing Modulus T from a Single Specimen Test Record," in *Fracture Mechanics*, ed. R. Roberts (West Conshohocken, PA: ASTM International, 1981), 476–502, <https://doi.org/10.1520/STP28814S>
7. M. H. Sharobeam and J. D. Landes, "The Load Separation Criterion and Methodology in Ductile Fracture Mechanics," *International Journal of Fracture* 47, no. 2 (January 1991): 81–104, <https://doi.org/10.1007/BF00032571>
8. M. H. Sharobeam and J. D. Landes, "The Load Separation and η_{pl} Development in Precracked Specimen Test Records," *International Journal of Fracture* 59, no. 3 (February 1993): 213–226, <https://doi.org/10.1007/BF02555184>
9. C. R. Bernal, A. N. Cassanelli, and P. M. Frontini, "A Simple Method for J-R Curve Determination in ABS Polymers," *Polymer Testing* 14, no. 1 (1995): 85–96, [https://doi.org/10.1016/0142-9418\(95\)90616-0](https://doi.org/10.1016/0142-9418(95)90616-0)
10. C. R. Bernal, A. N. Cassanelli, and P. M. Frontini, "On the Applicability of the Load Separation Criterion to Acrylonitrile/Butadiene/Styrene Terpolymer Resins," *Polymer* 37, no. 18 (September 1996): 4033–4039, [https://doi.org/10.1016/0032-3861\(96\)00232-7](https://doi.org/10.1016/0032-3861(96)00232-7)
11. C. R. Bernal, P. E. Montemartini, and P. M. Frontini, "The Use of Load Separation Criterion and Normalization Method in Ductile Fracture Characterization of Thermoplastic Polymers," *Journal of Polymer Science Part B: Polymer Physics* 34, no. 11 (August 1996): 1869–1880, [https://doi.org/10.1002/\(SICI\)1099-0488\(199608\)34:11<1869::AID-POLB4>3.0.CO;2-N](https://doi.org/10.1002/(SICI)1099-0488(199608)34:11<1869::AID-POLB4>3.0.CO;2-N)
12. C. Morhain and J. I. Velasco, "Determination of J-R Curve of Polypropylene Copolymers Using the Normalization Method," *Journal of Materials Science* 36, no. 6 (March 2001): 1487–1499, <https://doi.org/10.1023/A:1017500930544>
13. C. Morhain and J. I. Velasco, "J-R Curve Determination of Magnesium Hydroxide Filled Polypropylene Using the Normalization Method," *Journal of Materials Science* 37, no. 8 (April 2002): 1635–1644, <https://doi.org/10.1023/A:1014944729912>
14. A. Salazar and J. Rodríguez, "The Use of the Load Separation Parameter S_{pb} Method to Determine the J–R Curves of Polypropylenes," *Polymer Testing* 27, no. 8 (December 2008): 977–984, <https://doi.org/10.1016/j.polymertesting.2008.08.013>
15. F. Baldi, S. Agnelli, and T. Riccò, "On the Applicability of the Load Separation Criterion in Determining the Fracture Resistance (J_{IC}) of Ductile Polymers at Low and High Loading Rates," *International Journal of Fracture* 165, no. 1 (September 2010): 105–119, <https://doi.org/10.1007/s10704-010-9510-9>
16. F. Baldi, S. Agnelli, and T. Riccò, "On the Determination of the Point of Fracture Initiation by the Load Separation Criterion in J-Testing of Ductile Polymers," *Polymer Testing* 32, no. 8 (December 2013): 1326–1333, <https://doi.org/10.1016/j.polymertesting.2013.08.007>
17. A. Salazar, J. Rodríguez, F. Arbeiter, G. Pinter, and A. B. Martínez, "Fracture Toughness of High Density Polyethylene: Fatigue Pre-cracking versus Femtolaser, Razor Sharpening and Broaching," *Engineering Fracture Mechanics* 149 (November 2015): 199–213, <https://doi.org/10.1016/j.engfractmech.2015.07.016>
18. A. B. Martínez, A. Salazar, N. León, S. Illescas, and J. Rodríguez, "Influence of the Notch-Sharpening Technique on Styrene-Acrylonitrile Fracture Behavior," *Journal of Applied Polymer Science* 133, no. 32 (August 2016): 43775, <https://doi.org/10.1002/app.43775>
19. Y. Patel, B. R. K. Blackman, and J. G. Williams, "Determining Fracture Toughness from Cutting Tests on Polymers," *Engineering Fracture Mechanics* 76, no. 18 (December 2009): 2711–2730, <https://doi.org/10.1016/j.engfractmech.2009.07.019>
20. J. G. Williams, "Introduction to Linear Elastic Fracture Mechanics," in *Fracture Mechanics Testing Methods for Polymers Adhesives and Composites, European Structural Integrity Society Publication 28*, ed. D. R. Moore, A. Pavan, and J. G. Williams (Oxford, UK: Elsevier, 2001), 3–10.
21. J. G. Williams, *Fracture Mechanics of Polymers* (Chichester, UK: Ellis Horwood Limited, 1987).
22. J. R. Rice, P. C. Paris, and J. G. Merkle, "Some Further Results of J-Integral Analysis and Estimates," in *Progress in Flaw Growth and Fracture Toughness Testing*, ed. J. G. Kaufman, J. Swedlow, H. Corten, J. Srawley, R. Heyer, E. Wessel, and G. Irwin (West Conshohocken, PA: ASTM International, 1973), 231–245, <https://doi.org/10.1520/STP49643S>

23. F. Baldi and T. Riccò, "High-Rate J-Testing of Toughened Polyamide 6/6: Applicability of the Load Separation Criterion and the Normalization Method," *Engineering Fracture Mechanics* 72, no. 14 (September 2005): 2218–2231, <https://doi.org/10.1016/j.engfracmech.2005.02.002>
24. S. Agnelli, F. Baldi, L. Castellani, K. Pisoni, M. Vighi, and L. Laiarinandrasana, "Study of the Plastic Deformation Behaviour of Ductile Polymers: Use of the Material Key Curves," *Mechanics of Materials* 117 (February 2018): 105–115, <https://doi.org/10.1016/j.mechmat.2017.11.002>